Antiviral Research 84 (2009) 48–59

Contents lists available at ScienceDirect

Antiviral Research

journal homepage: www.elsevier.com/locate/antiviral

# Identification of allosteric inhibitors blocking the hepatitis C virus polymerase NS5B in the RNA synthesis initiation step

Stéphane Betzi[a,b,1,4], Cécilia Eydoux[c,d,4], Cécile Bussetta[c,d,2,4], Marilyne Blemont[c,d], Pieter Leyssen[h], Claire Debarnot[c,d], Mohamed Ben-Rahou[c,d], Jacques Haiech[e], Marcel Hibert[e], Françoise Gueritte[f], David S. Grierson[g], Jean-Louis Romette[c,d], Jean-Claude Guillemot[c,d], Johan Neyts[h], Karine Alvarez[c,d], Xavier Morelli[a,b,*,5], Hélène Dutartre[d,**,3,5], Bruno Canard[c,d]

[a] *Centre National de la Recherche Scientifique (CNRS), Laboratoire IMR, FRE 3083, 31 Chemin Joseph Aiguier, 13402 Marseille cedex 20, France*
[b] *Université de Provence, 3 place Victor Hugo, 13001 Marseille cedex 3, France*
[c] *Université de la Méditerranée, 58 Bd Charles Livon, 13284 Marseille cedex 07, France*
[d] *AFMB-CNRS-UMR 6098, Department of Structural Virology, case 925, 163 avenue de Luminy, 13288 Marseille cedex 9, France*
[e] *Faculté de Pharmacie de Strasbourg, 74 route du Rhin, BP 24, 67401 Illkirch, France*
[f] *Institut de Chimie des Substances Naturelles ICSN-CNRS (UPR 2301), 91198 Gif-sur-yvette, France*
[g] *Institut Curie/CNRS, UMR 176, Bât. 110-112, Université Paris-Sud, Orsay F-91405, France*
[h] *Rega Institute for Medical Research, Katholieke Universiteit Leuven, Minderbroedersstraat 10, B-3000 Leuven, Belgium*

ARTICLE INFO

*Article history:*
Received 8 March 2009
Received in revised form 23 June 2009
Accepted 26 June 2009

*Keywords:*
Polymerase
Hepatitis C virus
Inhibitor screening
Mechanism of inhibition
Antiviral

ABSTRACT

Hepatitis C virus (HCV) RNA-dependent RNA polymerase NS5B constitutes a target of choice for the development of anti-HCV drugs. Although many small molecules have been identified as allosteric inhibitors of NS5B, very few are active in clinical applications. We have screened 17,000 compounds in an enzymatic assay involving the purified NS5B in order to increase the therapeutic arsenal. We hoped to shed some light on the precise mechanism of RNA synthesis. We succeeded in isolating a series of 21 original inhibitors of the RNA synthesis by NS5B. Four of these non-nucleoside inhibitors (NNIs) could be mapped to the known binding site called 'B' as judged by the decrease in their inhibition potency when assayed with a 'B' site mutant, M423T NS5B. Incidentally, our *in silico* model pointed to Y477 as a key residue for inhibitor binding. *In vitro*, Y477F mutant loses its sensitivity to the newly discovered inhibitors but is unable to extend primers during the elongation phase. Our results demonstrate that elements of the 'B' site are involved in the conformational changes required in the switch between the different RNA synthesis steps and that compounds targeting this site could lock the enzyme in its initiation phase.


*Abbreviations:* HCV, hepatitis C virus; CMV, cytomegalovirus; HSV, herpes simplex virus; HBV, hepatitis B virus; dsRNA, double-stranded ribonucleic acid; ssRNA, single-stranded ribonucleic acid; RdRp, RNA-dependent RNA polymerase; WT, wild-type; GTP, guanosine triphosphate; NI(s), nucleoside inhibitor(s); NNI(s), non-nucleoside inhibitor(s); NS5B, non-structural protein 5B; $P_x$, products made of *x* nucleotides (where *x* is a number of nucleotides); neg, negative; pos, positive; DMSO, dimethyl sulfoxide; %, percentage; SBDD, structure-based drug design; PDB, Protein Data Bank; PDB ID, Protein Data Bank Identifier; LGA, Lamarckian genetic algorithm; RMSD, root-mean-square deviation; AU, arbitrary unit; $IC_{50}$, 50% inhibitory concentration; LIMS, laboratory information management system; SAR, structure–activity relationship; DTT, dithiothreitol; Mn, manganese; Mg, magnesium.

* Corresponding author. CNRS, IBSM, FRE 3083, 31 Chemin Joseph Aiguier, 13402 Marseille cedex 20, France. Tel.: +33 491 164 501; fax: +33 491 164 540.
** Corresponding author. Baylor Institute for Immunological Research, 3434 Live Oak St, Dallas, TX 75204, USA. Tel.: +1 214 820 8929; fax: +1 214 820 4813.
*E-mail addresses:* morelli@ibsm.cnrs-mrs.fr (X. Morelli), helene.dutartre@baylorhealth.edu (H. Dutartre).
[1] Moffitt Cancer Center and Research Institute, 12902 Magnolia Drive, Tampa, FL 33612, USA.
[2] University of Texas Medical Branch, Department of Biochemistry and Molecular Biology, 301 University Boulevard, Galveston, TX 77555, USA.
[3] Baylor Institute for Immunological Research, 3434 live Oak St, Dallas, TX 75204, USA.
[4] These authors contributed equally to this work as first authors.
[5] These authors contributed equally to this work as senior authors.

0166-3542/$ – see front matter © 2009 Elsevier B.V. All rights reserved.
doi:10.1016/j.antiviral.2009.06.009

## 1. Introduction

Hepatitis C virus (HCV) infection has emerged as one of the most significant disease to affect humans. HCV is responsible for acute and chronic hepatitis that could lead to cirrhosis and/or liver cancer (http://www.who.int/en/). Currently, more than 170 million people are infected with HCV around the world with 3–4 million new infections each year. Despite its large medical and economical impact, there are no vaccines or efficient therapies without major side effects. Indeed, current antiviral therapies rely on the association of pegylated alpha-interferon with the nucleoside analogue Ribavirin and its efficiency depends upon HCV genotype, the non-1 genotypes being the easier to treat (Somsouk et al., 2003). Viral polymerases, essential for viral replication, are significant targets for therapeutic intervention. The use of inhibitors against viral polymerases has current clinical applications in the treatment of infections with different viruses such as human immunodeficiency virus (HIV); cytomegalovirus (CMV); herpes simplex virus (HSV); hepatitis B virus (HBV). The HCV non-structural protein 5B (NS5B) is the RNA-dependent RNA polymerase responsible for the complete copy of the RNA viral genome. *In vivo*, this reaction is thought to start without a primer (*de novo* RNA synthesis (Butcher et al., 2001; Luo et al., 2000)), meaning that the polymerase must synthesize its own dinucleotide primer in a process referred to as "initiation phase". The polymerase then elongates this primer until the end of the template in a process referred to as the "elongation phase".

From a structural point of view, the *de novo* replication implies that the enzyme adopts at least two different conformations. However, the various PDB-deposited three-dimensional structures are representative of only one conformation proposed to be the one adopted during the initiation phase (Ng et al., 2008).

From a biochemical point of view, RNA synthesis can be divided into different steps directly linked to the enzyme conformational stages. Three steps can be identified through the appearance of abortive synthesis RNA products of several sizes, in addition to the template size product: (1) a non-rate-limiting initiation step (formation of products made of 2 nucleotides: $P_2$); (2) a rate-limiting step for the formation of $P_3$–$P_6$ (first and second conformational changes?); (3) a non-rate-limiting final elongation from the $P_6$ product to the template-sized product (Dutartre et al., 2005). Step 1 may be regarded as the initiation phase, step 2 as the transition phase and step 3 as the elongation phase. In theory, polymerase inhibitors could potentially target all these steps either by acting at one or several of them.

HCV polymerase inhibitors can be classified into two classes: nucleoside inhibitors (NIs) and non-nucleoside inhibitors (NNIs). NIs are modified nucleosides, which, once activated to the 5′-triphosphate form, can be used as substrates at the polymerase active site to compete with natural nucleotides (Fig. 1, 'X' site), acting as non-obligate chain terminators after incorporation into the nascent RNA. Depending on the nature of the 2′ modification, 2′-Me or 2′-O-Me, NIs are active respectively at both initiation and elongation phases, or at the initiation phase only (Dutartre et al., 2005, 2006).

On the other hand, NNIs are diverse small molecules. They are non-competitive inhibitors that target the alloenzyme free of substrate and uncomplexed with any other non-structural replicative proteins. They are inactive when the enzyme has entered the processive RNA elongation phase (Beaulieu, 2007; Ma et al., 2005), which suggests that they target preferentially the initiation phase of the reaction. The combination of crystallographic, biochemical and mutagenesis studies allowed the identification of four NNI binding sites at the NS5B surface (for review, see De Francesco and Migliaccio (2005)). 'A' and 'B' sites are located in the thumb domain (Fig. 1, 'A' and 'B' sites), while 'C' and 'D' sites partially overlap between the thumb and the palm in a close proximity to the active site (Fig. 1, 'C' and 'D' sites).

Although very promising *in vitro*, most of these NNIs provided unsatisfactory results in clinical trials and new generation of compounds is still under phase I clinical evaluation. This is mainly due to either adverse side effects, rapid selection of virus mutant leading to resistance (http://www.hcvadvocate.org/hepatitis/hepC/HCVDrugs.html), or naturally occurring polymorphism in the polymerase 'B' site or

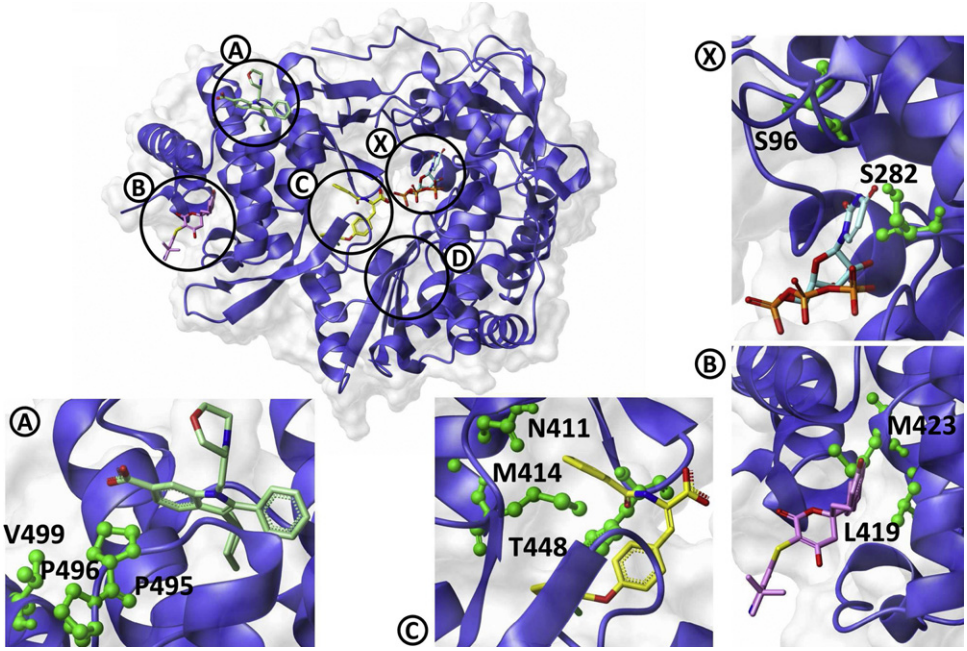


**Fig. 1.** HCV RNA-dependent RNA polymerase. Three-dimensional structure of HCV NS5B with locations of the four allosteric sites ('A', 'B', 'C' and 'D') and the active site ('X'). Zoom details present the binding of inhibitors to each allosteric site (except for the 'D' site) and the binding of UTP in the active site. Green balls and sticks residues also present several resistance mutations that protect the enzyme from inhibitor susceptibility. Structural data for 'X', 'A', 'B', and 'C' sites come from several PDB structure files: 1GX6 (Bressanelli et al., 2002), 2BRK (Di Marco et al., 2005), 1OS5 (Love et al., 2003) and 1YVF (Pfefferkorn et al., 2005), respectively.

'C' site among the different genotypes (Ludmerer et al., 2005; Pauwels et al., 2007). Therefore, efforts to increase the potency of these NNIs are needed either through structure-based drug design approach (SBDD), structure–activity relationship (SAR) studies and chemical modifications (Beaulieu, 2007; Biswal et al., 2006; Ikegashira et al., 2006; Koch et al., 2006; Lee et al., 2006; Powers et al., 2006). Meanwhile, screening campaigns with original compound libraries are also ongoing with the hope to discover new active lead compounds.

In this manuscript, we have identified 21 original NS5B NNIs using an enzyme-based screening of the French national library. Among them, a subset of NNIs that shares a same 6-xanthone chemical motif was the most efficient with $IC_{50}$ values in the micromolar range. Using point mutants we have mapped the location of the 6-xanthone derivatives to the allosteric 'B' site. We have then generated the computer-docking poses of these original inhibitors in the allosteric 'B' site. These predictions identified series of unexpected binding interactions. Indeed, several amino acids putatively involved were not previously described as key residues of allosteric 'B' site. When Tyrosine 477 was mutated to Phenylalanine (Y477F), the purified NS5B actively synthesized the 5′-triphosphate dinucleotide but was insensitive to the inhibitors, confirming the role of tyrosine in the binding of these 6-xanthone derivatives. Surprisingly, the Y477F NS5B was unable to engage the polymerase into the elongation phase, indicating that this residue is critical in a structural transition of the enzyme in the early step of RNA synthesis.

## 2. Materials and methods

### 2.1. HCV 1b polymerase plasmid constructs, enzyme preparation, and reagents

WT or mutant NS5B-Δ55 genes were tagged by six C-terminal histidine residues and expressed from the pDest 14 vector (Invitrogen) in *E. coli* BL21 (DE3) cells (Novagen). Site-directed mutagenesis was performed using the Quick Site-directed mutagenesis kit according to the manufacturer's instructions (Stratagene). All constructs were verified by DNA sequencing. WT, M423T, M414T, Y477F or R501A NS5B were produced and purified as previously described (Dutartre et al., 2005). DNA oligonucleotides were obtained from Lifetechnologies, homopolymeric cytosine (poly(C)) RNA template was obtained from Amersham-Pharmacia, and the 15-mer poly(C) RNA oligonucleotide template was purchased from Dharmacon. Uniformly labeled [$^3$H]-GTP (5.20 Ci/mmol) and [α-$^{32}$P]-GTP (3000 Ci/mmol) was purchased from Amersham-Bioscience.

### 2.2. Enzymatic activity assay of the HCV polymerase

Polymerase activity was assayed by monitoring the incorporation of radiolabeled guanosine into 15-mer oligo(C) RNA oligonucleotide templates or into a homopolymeric poly(C) RNA template, as previously described (Dutartre et al., 2005). To identify the inhibition type and the $K_i$ values, various concentrations of GTP (from 25 to 250 μM) or RNA template (from 4 to 20 nM) were tested without and with 1, 2 and 5 μM of compound **11** in the polymerase assay (Dutartre et al., 2005). The reaction time course was followed from 1 to 15 min. The initial velocity for each condition was used to draw a reciprocal Lineweaver–Burke plot and Dixon plots to determine the $K_i$ and $K_i'$ values.

### 2.3. Fluorescence measurements

Fluorescence was measured using a Tecan Saphire$^2$ spectrophotometer. All measurements were performed in Greiner 96-well microtiterplates (flat bottom black) from Nunc. In each well, 250 nM of WT, Y477F or R501A NS5B were assayed in 50 mM Hepes pH 8.0; 10 mM KCl; 1 mM $MgCl_2$; 10 mM DTT; 2 mM $MnCl_2$. Fluorescence spectra were recorded at an excitation wavelength of 290 nm and emission was monitored from 310 nm to 400 nm, with a step of 5 nm. Subtracting the buffer signal from the signal eliminated background emission. Each result was from the average of four independent measurements. Intra-assay variability was also determined by evaluating the same sample four times within the same assay run (%CV = (SD/mean) × 100, where CV = coefficient of variation, and SD = standard deviation). Inter-assay variability was determined by evaluating the samples in four consecutive assay runs (%CV = (SD/mean) × 100).

### 2.4. Evaluation of antiviral activity and cytostatic activities of selected compounds in HCV genotype 1b subgenomic replicon carrying Huh-5-2 cells

Huh-5-2 cells were cultured in RPMI medium (GIBCO) supplemented with 10% fetal calf serum, 2 mM L-glutamine (Life Technologies), 1× non-essential amino acids (Life Technologies); 100 IU/mL penicillin and 100 μg/mL streptomycin and 250 μg/mL G418 (Geneticin, Life Technologies). Cells were seeded at a density of 7000 cells per well in 96-well View PlateTM (Packard) in medium containing the same components as described above, except for G418. Cells were allowed to adhere and proliferate for 24 h. At that time, culture medium was removed and five serial dilutions (5-fold dilutions starting at 50 μg/mL or around 60 μM) of the test compounds were added in culture medium lacking G418. Interferon alfa 2a (500 IU) was included as a positive control in each experiment for internal validation. Plates were further incubated at 37 °C and 5% $CO_2$ for 72 h. Replication of the HCV replicon in Huh-5-2 cells results in luciferase activity in the cells. Luciferase activity was measured by adding 50 μL of 1× Glo-lysis buffer (Promega) for 15 min followed by 50 μL of the Steady-Glo Luciferase assay reagent (Promega). Luciferase activity was measured with a luminometer and the signal in each individual well is expressed as a percentage of the untreated cultures. The 50% effective concentrations ($EC_{50}$) were calculated from these datasets. Parallel cultures of Huh-5-2 cells, seeded at a density of 7000 cells/well of classical 96-well cell culture plates (Becton-Dickinson) were treated in a similar fashion except that no Glo-lysis buffer or Steady-Glo Luciferase reagent was added. The effect of the compounds on the proliferation of the cells was measured 3 days after the addition of the various compounds by means of The CellTiter 96® AQueous Non-Radioactive Cell Proliferation Assay (MTS, Promega). In this assay 3-(4,5-dimethylthiazol-2-yl)-5-(3-carboxymethoxyphenyl)-2-(4-sulfophenyl)-2H-tetrazolium (MTS) is bioreduced by cells into a formazan that is soluble in tissue. The number of cells correlates directly with the production of the formazan. The MTS stained cultures were quantified in a plate reader.

### 2.5. Library screening

The screening campaign was conducted using a chemical library made of 17,000 molecules originating from the French National Library, and completed by the Prestwick commercial library and the "Diversity" library from the National Cancer Institute (NCI). Quality of measurements was assessed by calculating the $Z'$ factor for each plate:

$Z'$ factor = $1 - ((3SD(neg) + 3SD(pos))/(avg(neg) - avg(pos)))$, where SD(neg) and SD(pos) stand for the standard deviation obtained for negative and positive controls, respectively, and where avg(neg) and avg(pos) are averages for negative and positive controls, respectively. The $Z'$ factor had an average value of 0.834 with a standard deviation of 0.058 for assay plates indicating that there is a wide separation of data points between the baseline and positive signals. For each compound, the percentage of inhibition

was calculated as follows:

$$\text{Inhibition}\,\% = 100(\text{raw\_data\_of\_compound} - \text{avg(pos)}/(\text{avg(neg)} - \text{avg(pos)})$$

The library was organized in 220 plates (96-well), each containing 80 compounds. Assay plates contained positive and negative controls distributed in the first and 12th columns, respectively. The library compounds from the French National Library included molecules coming from the ICSN-CNRS (UPR2301) (Gif-sur-Yvette), the UMR 176 CNRS/Institut Curie laboratory (Paris), and the UMR 7081 CNRS-University of Strasbourg (Illkirch, France). Details can be found at http://chimiotheque-nationale.enscm.fr/. The library also contained compounds from the Prestwick commercial library (http://www.prestwickchemical.fr) and from the "Diversity" library from the National Cancer Institute (http://dtp.nci.nih.gov/branches/dscb/diversity_explanation.html). Our experimental screening consisted of an *in vitro* nucleotide incorporation assay in which a functionally active recombinant NS5B enzyme and a homopolymeric poly(C) template were used. Reactions were conducted in 20 μL volume. Positive and negative controls consisted of an enzyme mix (50 mM HEPES pH 8.0, 10 mM KCl, 2 mM $MnCl_2$, 1 mM $MgCl_2$, 10 mM DTT, 0.5% Igepal CA630, 100 nM of homopolymeric poly(C) RNA template, 0.1 μM of NS5B) supplemented by 0.1 mM [$^3$H]-GTP (0.5 μCi) and 5% DMSO or 10 mM EDTA, respectively. For each assay, the enzyme mix was first distributed in plate wells using a BioMek 3000 automate (Beckman). Each 80 compounds was then added to the assay using a BioMek NX automate (Beckman) to a final concentration of 50 μM in 5% DMSO. Reactions were initiated by the addition of 0.1 mM [$^3$H]-GTP (0.5 μCi), incubated at 30 °C, and stopped after 20 min by the addition of EDTA (50 mM final concentration). All distributions were conducted with the Biomek 3000 automate. Reaction products were then transferred onto DE-81 paper membrane (Whatman International Ltd.) with a Packard Filtermate® Harvester. Filter paper membranes were washed three times in 0.3 M ammonium formate, pH 8.0, washed two times in ethanol, and dried. The radioactivity bound to the filter was determined using liquid scintillation counting (Wallac Microbeta® Trilux). After determining the percentage of inhibition, data were stored and managed using the LIMS software provided by ModulBio® (Marseille). Compounds showing 80% or more of reaction inhibition were selected and used to generate new experimental plates. These experimental plates were used for a second screen at a 10 μM final concentration, with the same experimental procedure. Compounds leading to 80% inhibition or more in the second screen were qualified as hits. Hits were then confirmed on purified freshly solubilized compound and $IC_{50}$ values were determined.

### 2.6. Inhibitory concentration of 50% of the reaction ($IC_{50}$)

The compound concentration leading to 50% inhibition of NS5B-mediated RNA synthesis was determined in RdRp buffer (cf. library screening section) containing 100 nM of homopolymeric poly(C) RNA template, 0.1 μM of NS5B and various concentrations of compound (from 250 μM to 2.1 μM or 35 μM to 0.29 μM depending of the initial percentage of inhibition). Reactions incubated at 30 °C were initiated by the addition of 0.1 mM [$^3$H]-GTP (0.5 μCi), and stopped after 20 min by the addition of EDTA (50 mM final concentration). Reaction products were transferred onto DE-81 paper membrane (Whatman International Ltd.) with a Packard Filtermate® Harvester. Filter paper membranes were washed three times in 0.3 M ammonium formate, pH 8.0, two times in ethanol, and dried. Radioactivity bound to filters was determined using liquid scintillation counting (Wallac Microbeta® Trilux). $IC_{50}$ was determined using the equation: % of active enzyme = $100/(1+(I)^2/IC_{50})$, where $I$ is the concentration of inhibitor. $IC_{50}$ was determined from curve-fitting using Kaleidagraph (Synergy Software). For each value, results were obtained using triplicate in a single experiment. Final $IC_{50}$ values were calculated by the average of two independent experiments.

### 2.7. Definition of the active site and docking parameters for FlexX and AutoDock

A structure-based drug design (SBDD) approach was applied on the 2.2 Å resolution crystallographic structure of the HCV polymerase in complex with a competitive inhibitor NH1 (Love et al., 2003) (PDB ID: 1OS5). We selected two docking programs and several scoring functions for docking experiments: FlexX 2.0 (Kramer et al., 1999) with the five scoring functions of the Cscore™ Sybyl™ module (Clark et al., 2002): FlexXscore, Gscore, Dscore, PMFscore, Chemscore (http://www.biosolveit.de), and AutoDock 3.0 using its own scoring function (Morris et al., 1996). We also re-scored each docking with our in house scoring function, GFscore (http://gfscore.cnrs-mrs.fr) (Betzi et al., 2006).

TRIPOS Sybyl "Structure Preparation Tool" was used to optimize the protein structure before use by FlexX 2.0. Hydrogen atoms were added, bumps and side chain amides were then corrected, and finally missing residues were added and minimized. The newly obtained PDB file was then injected as such in FlexX 2.0.

For each docking program, the "active site" used for the docking is always composed of a pocket containing all atoms of NS5B no farther than 6.5 Å of the NH1 crystalline position. The best parameters were evaluated for each docking program according to their ability to mimic the crystallographic pose of the NH1 ligand (we formerly corrected the NH1 structure and atom valences according to the NCBI Pubchem structural data server (http://pubchem.ncbi.nlm.nih.gov/).

### 2.8. Docking with AutoDock 3.0

Prior to the docking studies, crystallographic ligands and water molecules were removed. Polar hydrogen atoms were added and Kollman charges were assigned to all atoms. The docking site was defined within a box around residues of the binding site. For each kind of ligand atoms, 50 Å × 50 Å × 60 Å 3D grids centered on the binding site with 0.375 Å spacing were calculated using Autogrid3 (Morris et al., 1996). For docking simulations, we selected the Lamarckian genetic algorithm (LGA) for ligand conformational searching because it has enhanced performance relative to simulated annealing or the simple genetic algorithm. The program uses a five-term force field-based function derived from the AMBER force field, and that comprises a Lennard-Jones 12-6 dispersion term, a directional 12-10 hydrogen bonding term, a coulombic electrostatic potential, an entropic term, and an intermolecular pair-wise desolvation term. The scaling factor for each of these five terms is empirically calibrated from a set of 30 structurally known protein–ligand complexes.

The ligand translation, rotation, and internal torsions are defined as its state variables, and each gene represents a state variable. LGA adds local minimization to the genetic algorithm, enabling modification of the gene population. For each compound, we used the default docking parameters with the exception of the following: trials of 100 dockings, population size of 50, random starting position and conformation, and 250,000 energy evaluations. Final docked conformations were clustered using a tolerance of 1 Å root-mean-square deviation (RMSD).

### 2.9. Docking with FlexX 2.0

FlexX 2.0 is an incremental construction-docking algorithm involving three steps. FlexX cuts ligand into fragments, places the best one in binding site, and then makes an incremental construction of the whole ligand. Conformational flexibility of the ligand is taken into account by considering both torsion angle flexibility and conformational flexibility of ring systems (Rarey et al., 1996). FlexX by itself does not recognize the receptor flexibility; rather it sees proteins as rigid elements (bodies). Default FlexX parameters were used, as supplied in the TRIPOS Sybyl7.3.1 package, for carrying out flexible docking with 30 conformations for each molecule, using the place particle option as defined by Rarey et al. (1999). We also adjusted protonation state of the "Receptor Descriptor File" residues to protonated Lysine and Arginine residues and to ionized Aspartic and Glutamic acids residues.

## 3. Results

### 3.1. Isolation of inhibitors

Compounds showing RNA synthesis inhibition higher than 80% were selected in a screening campaign conducted at a 50 μM compound concentration and submitted to a second screening round at a 10 μM concentration. Twenty-one compounds identified as hits in the screening campaign were subjected to confirmation on a freshly prepared compound solution (from the original powder) and then to $IC_{50}$ determination in triplicate. Results are the average of two independent experiments (supplementary data). The $IC_{50}$ values were comprised between $1.1 \pm 0.1$ μM and $38.9 \pm 2.3$ μM. Compounds can be classified in four families based on their chemical structure. The first family comprises three tetracycline derivatives (supplementary data, compounds **1**–**3**). The second, five compounds containing a xanthene chemical motif (supplementary data, compounds **7**–**11**) and among them 4 share the same 6-xanthone motif (compounds **8**–**11**). The third comprises two compounds bearing the chalcone chemical motif (supplementary data, compounds **13** and **14**). Compounds with no obvious chemical relatedness are in the last family (supplementary data, compounds **4**, **12**, **15**–**21**). Out of the 21 hits, 6-xanthone derivatives showed the lowest $IC_{50}$, comprised between $1.1 \pm 0.1$ μM and $2.9 \pm 0.3$ μM. We then tested the 6-xanthone compound in HCV replicon expressing cells. Compound **11** showed a 68% inhibition of the HCV replicon when used at 10 μg/ml, with no toxicity measured by cell metabolism (100% of cell metabolism) observed at this concentration, leading to an $EC_{50}$ of about 5 μg/ml (8 μM). However, at 50 μg/ml of compound **11**, cell viability was reduced to 17%, but 100% inhibition of the replicon was observed (data not shown). These data suggested that the activity of compound **11** against HCV replication is associated with cellular toxicity at higher doses that did not permit to conclude on a clear mechanism of action. Thus, we focused our effort on a rational approach coupling biochemistry and molecular modeling to further characterize the 6-xanthone and evaluate their potential interest as HCV polymerase inhibitors.

### 3.2. Determination of inhibitor binding sites

In order to determine the binding site of selected hits, we analyzed their inhibition properties on NS5B bearing a mutation reported to define each binding site (for a review, see De Francesco and Migliaccio (2005)). These three binding sites are located at the surface of the thumb domain (Fig. 1, 'A', 'B' and 'C' sites). Each single mutation has been reported to decrease binding of the inhibitor thus accounting for resistance (reviewed in De Francesco and Carfi (2007)). For the allosteric binding 'C' site, several different single mutations have been reported, but only the M414T mutation demonstrated a clear and universal resistance to the inhibitors that target this site. For the allosteric 'B' site, the M423T mutation is reported, so far, to be able to discriminate all inhibitors targeting this site (Pauwels et al., 2007). For the allosteric 'A' site, it has been reported that mutant polymerase bearing the P495L mutation are barely active *in vitro* (Dutartre et al., 2005). Indeed, when tested in our screening assay, the P495L mutant polymerase showed maximum activity only at 5% of that of WT (not shown), that rendered it unsuitable for further characterization of our 6-xanthone hits. However, the M423T, and M414T mutant polymerase genes were constructed and expressed *in vitro*. The polymerases were then purified and their activity compared to that of WT polymerase (Fig. 2). All protein samples were normalized to an apparent same concentration and degree of purity between each other (Fig. 2A). The M414T and M423T mutants exhibited similar activities although 2-fold decreased compared to that of WT enzyme (Fig. 2B), as already reported by others (Nicolas et al., 2008). We then determined $IC_{50}$ of the selected hits for the M423T or the M414T mutants (Table 1). All four 6-xanthone compounds (compounds **8**–**11**) showed a reproducible 2-fold $IC_{50}$ increase measured with the M423T mutant only, while the M414T mutant showed the same $IC_{50}$ as the WT enzyme (Table 1). Although low, this

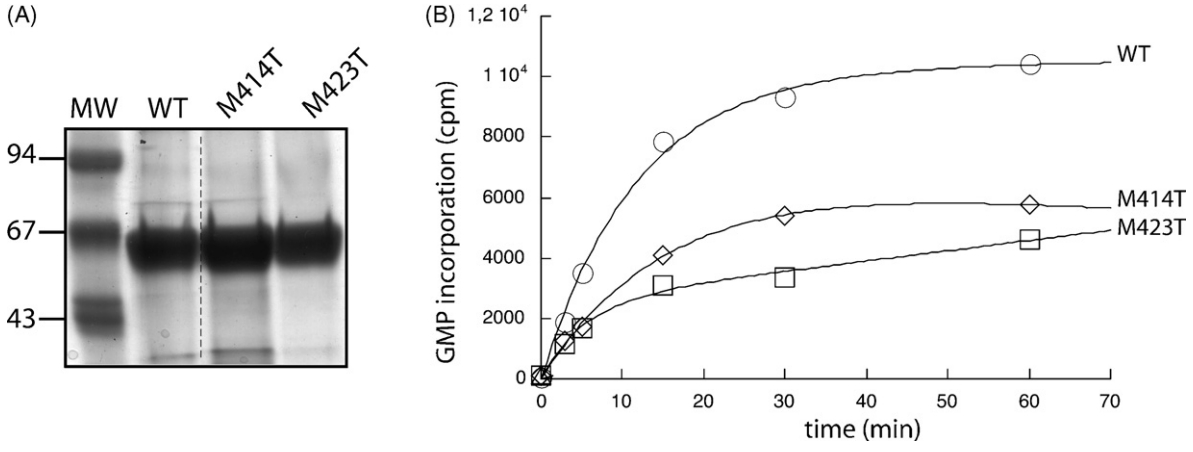


**Fig. 2.** Purification and activity of WT, M423T and M414T NS5B. (A) Purified NS5B proteins after a two-step purification procedure. The identity of each protein is given above the panel. A low-molecular weight marker (MW) corresponding to 94, 67 and 43 kDa is shown on the left. (B) Time course of incorporation of [$^3$H]GTP into poly(C) RNA template by WT (○) or M423T (□), M414T (◊) NS5B. RNA synthesis, analyzed by counting radiolabeled RNA spotted onto DE 81 paper disc, is represented as GMP incorporation into insoluble product (cpm) as a function of time.

**Table 1**
Structures and $IC_{50}$ values of the 6-xanthone compounds.

| Structure | $IC_{50}$ for WT (μM) | $IC_{50}$ for M423T (μM) | $IC_{50}$ for M414T (μM) | Number |
|---|---|---|---|---|
| 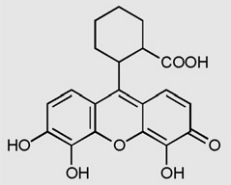 | 2.2 ± 0.4 | **4.7 ± 0.2** | 2.0 ± 0.1 | **08** |
| 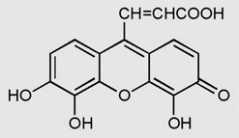 | 2.9 ± 0.3 | **4.9 ± 0.2** | 1.2 ± 0.1 | **09** |
| 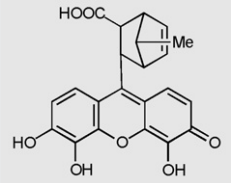 | 1.1 ± 0.1 | **2.9 ± 0.1** | 1.1 ± 0.05 | **10** |
| 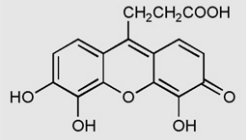 | 1.65 ± 0.08 | **3.65 ± 0.1** | 1.09 ± 0.08 | **11** |

Compounds found as inhibitors of WT, M423T or M414T NS5B after the *in vitro* screening are ranked according to their chemical structure similarity.

$IC_{50}$ change was still significant since it was reproduced in at least two independent experiments conducted each in triplicates, and using several aliquots of compounds. Moreover, error values calculated for the four identified 6-xanthone hits are low and thus fully acceptable as comprised between 0.05 μM and 0.2 μM. Finally, $IC_{50}$ curves showed complete inhibition of the enzyme activities at high concentrations of inhibitors (not shown). All together, these results make us confident in the reliability of the inhibition decrease observed with the mutants, and allowed to discriminate the binding site for 6-xanthone hits.

### 3.3. Mechanism of inhibition by 6-xanthone compounds

NNIs targeting the 'A' or 'C' sites can only bind the apo-enzyme (Pauwels et al., 2007; Tomei et al., 2003, 2004). They act by preventing either the interaction of the fingertip with the thumb (for 'A' site inhibitors (Di Marco et al., 2005)) or the exit of the neo-synthesized dsRNA (for 'C' site inhibitors (Pauwels et al., 2007)). In both cases, they freeze the enzyme in its RNA synthesis initiation conformation when the first phosphodiester bond formation occurs. In contrast, the mechanism of inhibition of 'B' site NNI binders is not yet understood and poorly documented. We first determined the type of inhibition by analyzing the compound behavior toward the nucleotides or RNA substrates. We determined the inhibition constant values $K_i$ and $K_i'$ in an enzymatic assay by using increasing concentration of GTP or RNA substrates in the presence of several concentrations of compound #11 (0, 1 and 5 μM for experiments with GTP and 0, 1, 2 and 5 μM for experiments with RNA) in the homopolymeric test of enzyme activity. Both Lineweaver–Burke and Dixon representations of the results showed a non-competitive inhibition to both GTP and RNA with the same values for $K_i$ and $K_i'$ of 1.1 ± 0.15 μM and 1 ± 0.2 μM for GTP and RNA, respectively (not shown). We then investigated which step of the RNA synthesis is affected by our 'B' site 6-xanthone inhibitors (compound **11**, Table 1) by analyzing the reaction products using a gel assay (Fig. 3). For this purpose, the polymerization reaction was performed using an oligo(C) template and GTP as the unique source of nucleotide. After electrophoresis, the products profile reflects the three RNA synthesis steps (Dutartre et al., 2005). As shown in Fig. 3, the 6-xanthone inhibitor compound **11** decreased the amount of all RNA products. Moreover, quantification of each band allowed determining an $IC_{50}$ value of about 1.5 μM in the vicinity to the value measured during the library screen (compounds **8**–**11** in Table 1 and supplementary data). However, when each band was analyzed separately as a marker for initiation ($G_2$ dinucleotide products), transition ($G_3$ to $G_6$ products) or elongation (template size products), no differential disappearance could be detected irrespective of the concentration of inhibitor used. This suggests that 6-xanthone compounds have no selectivity, acting on both initiation and elongation equally. Alternatively, the compounds could preferentially inhibit the initiation step of RNA synthesis, and thus impact consecutively RNA elongation. In order to understand the compounds mechanism of action, we examined their putative binding mode using molecular docking.

### 3.4. Molecular modeling and analysis of the 3-xanthone derivatives binding

We used two different docking programs, FlexX and AutoDock, to understand how the 6-xanthone compounds could bind the allosteric 'B' site. These two programs, based on different algorithms, allow eliminating any bias while generating the binding models. The lowest energy docking models were then selected using several scoring functions for further analysis. Docking models

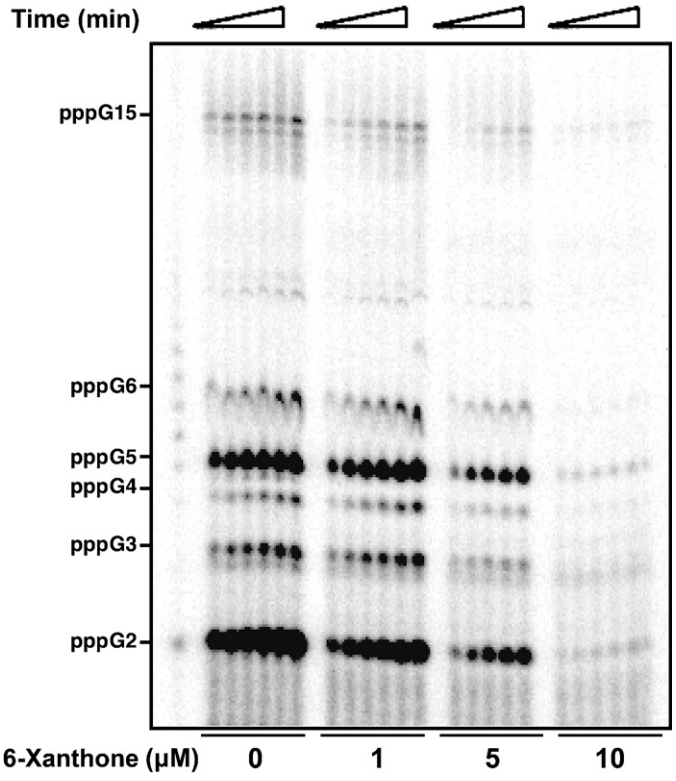


**Fig. 3.** 6-Xanthone derivatives inhibit WT NS5B-mediated RNA synthesis. Time course of incorporation of GMP into RNA using an oligo©RNA template. Reactions were performed as described in Section 2 using $\alpha$-$^{32}$P-GTP (1 $\mu$Ci), WT NS5B (500 nM) and 6-xanthone compound 11 (0, 1, 5, 10 $\mu$M). The reaction time course was followed from 30 s to 15 min. RNA products were resolved using 14% acrylamide denaturing gel electrophoresis. Positions of the RNA markers synthesized using T7 RNA polymerase are indicated on the left.

of these compounds were consistent using the two programs and were found very different compared to the reference compound (NH1 structure, PDB code 1OS5) (Fig. 1). NH1 makes hydrophobic contacts with the left side of the protein allosteric 'B' site, and is stabilized outside the groove with a few peripheral hydrogen bonds (Fig. 1, 'B' site; Fig. 4A and A′). NH1 is also involved in a sulfur-aromatic interaction with Methionine 423. On the contrary, the docking models generated using FlexX and AutoDock for the four new identified inhibitors suggested an interaction mode based on numerous hydrogen bonds at the center and right side of the 'B' site (Fig. 4B, B′ and Fig. 5). Two binding modes are proposed for the four 6-xanthone molecules (Table 1, compounds **8**–**11**). The first binding mode uses the right side of the active site with hydrogen bonds with residues Serine 473, Arginine 422 and Asparagine 527 (Fig. 5A), while the second binding mode uses the center part of the groove to define an extensive hydrogen bond network with Tyrosine 477, Arginine 422, Arginine 501 and Tryptophane 528 (Fig. 5B). In this model, an additional salt bridge involving Arginine 501 stabilizes the molecule.

Interestingly, on the left side of this groove, Methionine 423 (Fig. 4 and Fig. 5) is close to the docked compounds but does not make any interaction with it. This model is consistent with the observation that the M423T mutation modestly affects activity of the compounds in the *in vitro* assay. The model also suggests that another mutation might be better to exclude this compound from the allosteric site and foster a greater *in vitro* resistance.

In order to test this second putative binding model, four additional mutations were created in a central position of the 'B' site: Y477F, R501A, W528D and R422A.

### 3.5. Biochemical characterization of additional B site mutants

The Y477F, R501A, W528D and R422A mutants were constructed, expressed and purified with the protocol used for the WT expression. The W528D and R422A were not expressed to a suitable level, suggesting that these mutations significantly affected the conformation and/or stability of the corresponding proteins. Y477F and R501A could readily be purified to both similar amount and equivalent degree of purity as the WT protein (Fig. 6A). To check the correct folding of these mutants, we measured their intrinsic Tryptophan fluorescence. After excitation at $\lambda$ = 290 nm, an emission spectra could be recorded between $\lambda$ = 310 nm and $\lambda$ = 400 nm (Bougie et al., 2003) with a maximum fluorescence intensity of 700 arbitrary unit (AU) around $\lambda$ = 340 nm for the WT protein and the Y477F mutant (Fig. 6B). The maximum fluorescence intensity was decreased to 400 AU for the R501A mutant (Fig. 6B), and corresponded to the spectra of the protein denatured in 7 M urea (data not shown). This latter result suggests that the R501A mutant, although expressed to the same level as the WT protein, is mainly unfolded in solution. It also indirectly suggests that the integrity of the 'B' site might be critical for the correct folding of the protein. As expected from the fluorescence data, the R501A mutant was not active neither on homopolymeric poly(C) RNA template (Fig. 7A) nor using the oligo(C) template used as described earlier (Fig. 7B).

### 3.6. Inhibition of the Y477F mutant by 6-xanthone compounds

We next assessed the role of Tyrosine 477 in 6-xanthone binding by analyzing the inhibition of the Y477F mutant in the presence of increasing concentrations of 6-xanthone compound **11** (Fig. 8). Products of the polymerization synthesized using the oligo(C) template were analyzed using the denaturing gel assay in the presence of increasing concentration of 6-xanthone compound **11**. In contrast to what we observed for the WT enzyme (Fig. 3), the Y477F mutant was not affected by the 6-xanthone compound **11**, even at the highest concentration of 10 $\mu$M, i.e., 10-fold higher than the observed $IC_{50}$ using WT enzyme (Fig. 8). After quantification, we observed the same amount of $G_2$ dinucleotide products with all the concentrations of 6-xanthone used in this experiment. This result clearly indicates that the Y477F mutant loses its sensitivity to 6-xanthone compounds, and thus validates the second mode of binding proposed by the docking programs (Fig. 5B).

### 3.7. Tyrosine 477 as a trigger to the switch from initiation to elongation

The very conservative substitution of the Tyrosine 477 by a Phenylalanine did not affect expression or folding of the polymerase. However, the Y477F mutant enzyme was almost inactive when tested on a homopolymeric poly(C) template. Indeed, the maximum activity was only around 5% of WT enzyme activity (Fig. 7A). The products of the reaction were then examined using a gel assay (Fig. 7B): the synthesis of $G_2$ dinucleotide products was barely affected by the presence of Y477F, whereas a clear decrease in abundance for the products greater in size than $G_2$ was observed. We quantified each product separately and calculated the ratio of transition or elongated products from initiation products, in order to compare the percentage of switch to transition or to elongation for each enzyme (Table 2). These results showed that the switches to transition and elongation are decreased by 1.8-fold, and 1.6-fold respectively for the Y477F mutant enzyme compare to the WT enzyme, leading for the Y477F enzyme, to only 30% of the total RNA product synthesized by the WT enzyme (3-fold decrease of total elongated product (Table 2). This mutant was able to carry out the first phosphodiester bond formation, but was highly impaired in its capacity to proceed further. We con-

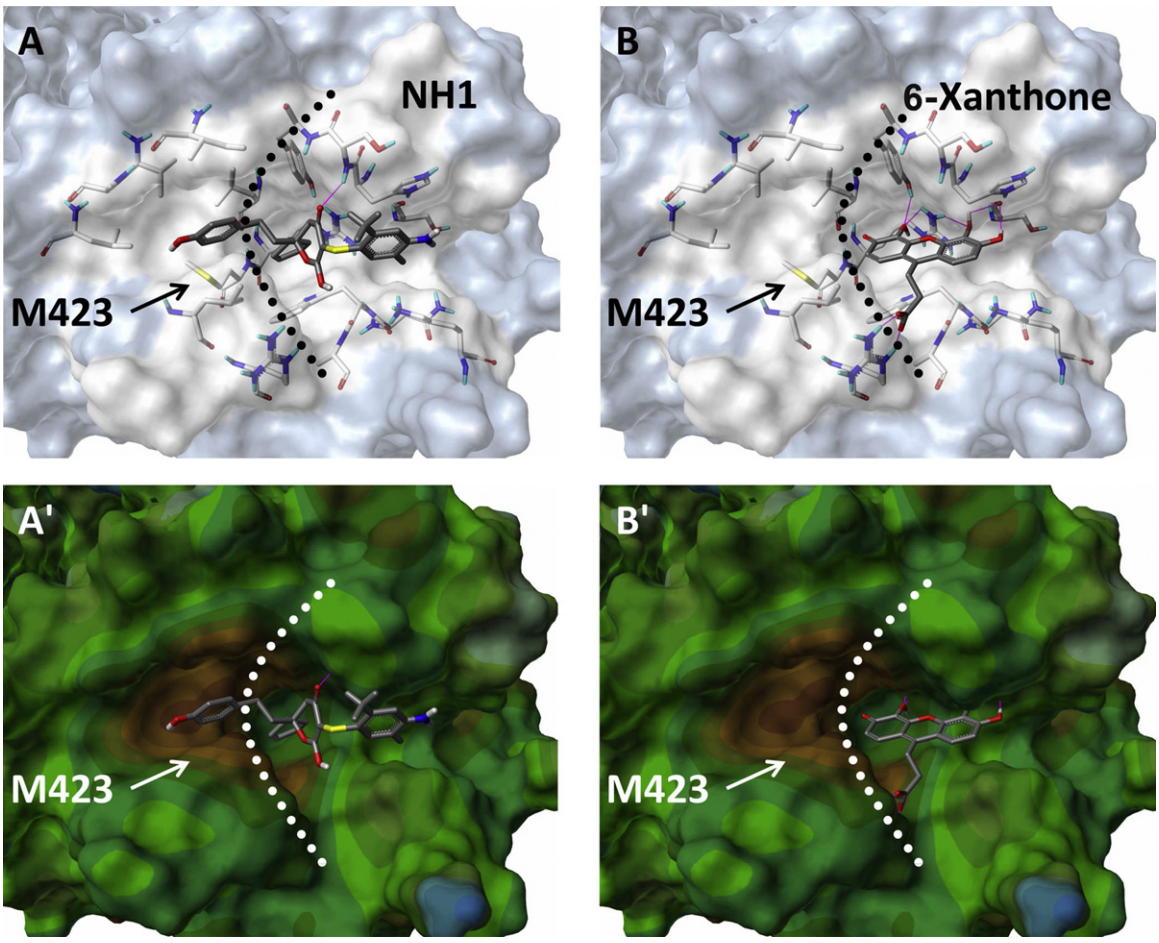


**Fig. 4.** Structural details of the binding of the NH1 inhibitor (PDB code 1OS5) compared to the FlexX docking model of a 6-xanthone compound. Each complex is shown with its hydrogen bond contacts in a stick representation (top) and a hydrophobic surface representation from blue (hydrophilic) to brown (hydrophobic (bottom). The cavity of the allosteric 'B' site is divided by a dot line separating a hydrophobic region (left part) and a polar region (right part). An aromatic ring of NH1 binds the hydrophobic left site of the groove (A and A′) while in the docking model, the 6-xanthone derivatives make several polar contacts with the center and the right side of the 'B' site (B and B′).

**Table 2**
Percentage of elongated products synthesized by WT and Y477F NS5b polymerases. The table shows the calculated percentage of transition product elongated from initiation (switch to transition); elongated product elongated from transition (switch to elongation) and the total elongated product from initiation products (switch initiation to elongation). Percentages were calculated based on the quantified initiation, transition or elongation products from Fig. 7B.

| | Switch to transition (I-T) (%) | Switch to elongation (T-E) (%) | Total elongated product (switch I-E) (%) |
|---|---|---|---|
| WT | 58 | 12.8 | 7.5 |
| Y477F | 32 | 7.8 | 2.5 |
| Fold decrease | 1.8× | 1.6× | 3× |

clude that Y477F alters the switch from initiation to transition and elongation.

## 4. Discussion

We have identified 21 inhibitors of NS5B-mediated RNA synthesis from the 17,000 compounds of the French national Library, complete with "Diversity" library of NCI and the Prestwick library. Among those, the 6-xanthone compound family was the most represented with $IC_{50}$ values around 1 μM. The leading compounds of this family, compound **11** was able to inhibit HCV replication in the HCV replicon-expressing cells, with an $EC_{50}$ of about 8 μM, similar to what we observed in *in vitro* polymerase experiments, but was associated with cellular toxicity at higher doses. This suggests that these compounds have some antiviral capacity that need to be chemically improved for their use *in vivo*, and justify our strategy to first better characterize their inhibition potency by a rational approach coupling biochemistry and molecular modeling. Using mutant polymerases specific to HCV polymerase allosteric binding sites, we observed a modest but reproducible increased in the $IC_{50}$ when polymerase activity was assayed with the M423T mutant, suggesting that 6-xanthone could target the 'B site'. As expected by its binding to an allosteric site, compound **11** acts as a non-competitive inhibitor with respect to nucleotides or RNA substrates with a $K_i$ constant inhibition values of about 1 μM (data not shown). Although probably identified as 'B' site binders by biochemical studies, molecular modeling analysis proposed very different binding modes for these new inhibitors compared to the binding mode of inhibitors previously described at this 'B' site (Love et al., 2003). All the newly generated binding modes suggest that they are driven by polar and electrostatic contacts at the right side and the central portion of the 'B' site. These models are in agreement with the observation that the M423T mutation provides only a modest resistance to these compounds. Indeed, the 'NH1' inhibitor-binding mode involves mostly hydrophobic contacts in the 'B' site cleft involving a cyclopentane group in the central position and a hydroxyphenyl group at the left involved in a sulfur-aromatic interaction with the Methionine 423 residue. The different docking models for 6-xanthone binding are distant from Methionine 423 and suggest that the M423T mutation might not properly impede 6-xanthone

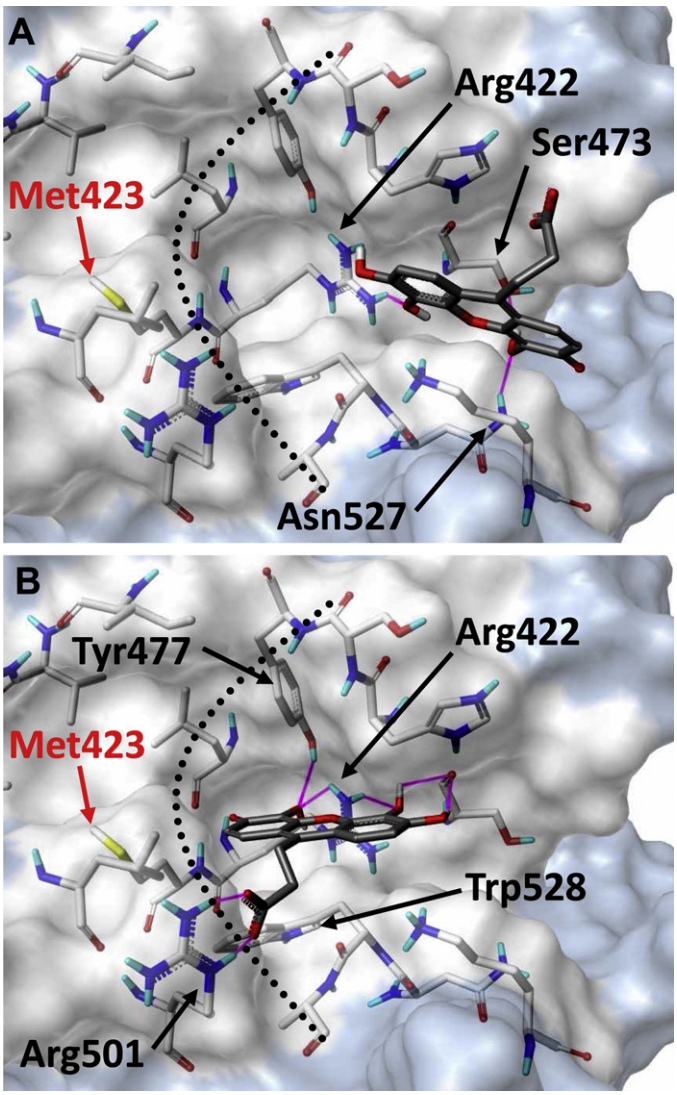


**Fig. 5.** Analysis of 6-xanthone derivatives FlexX binding models. Parts A and B represent two different binding models for the compound 11 6-xanthone derivative. Compounds **8** and **10** are preferentially docked as model A, in a right off-centered position involving few hydrogen bonds (hydrogen bonds are represented by purple lines), while compounds **9** and **11** fill preferentially the central cavity as in model B involving extensive hydrogen bond networks.

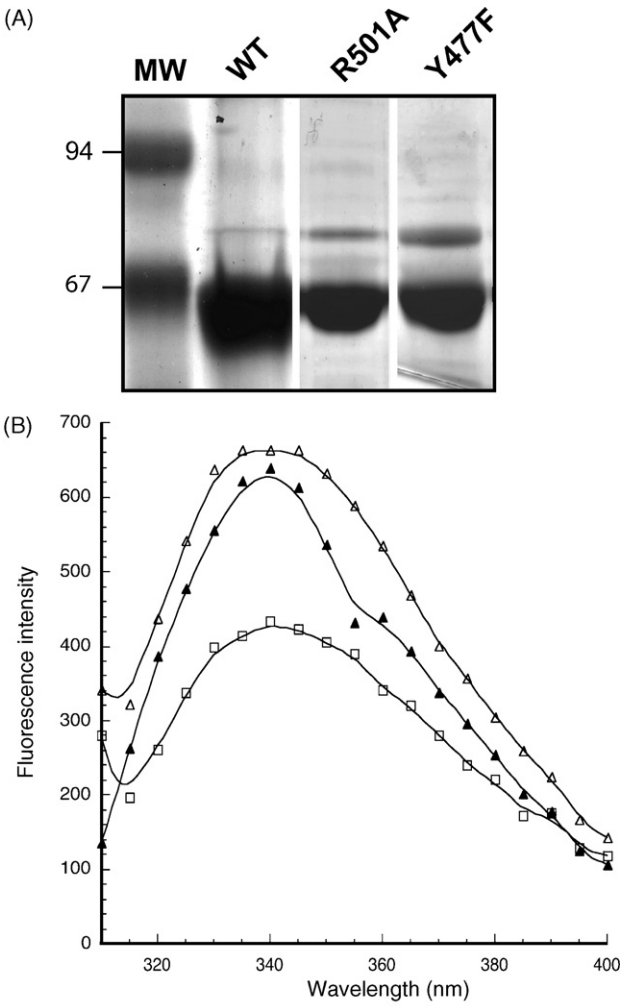


**Fig. 6.** Purification and folding analysis using fluorescence emission of the WT, Y477F and R501A NS5B proteins. (A) Purified NS5B proteins after a two-step purification procedure. The identity of each protein is given above. The low-molecular weight marker (MW) corresponding to 94 and 67 kDa is shown on the left. (B) Background corrected emission fluorescence spectra of NS5B WT (△) and Y477F (▲) or R501A (□) mutant polymerases. Fluorescence spectra were recorded at an excitation wavelength of 290 nm.

binding, in line with the *in vitro* inhibition data obtained in this study. This result is also interesting in light of the low structural conservation of the 'B' site related to its naturally occurring polymorphism (Pauwels et al., 2007). Indeed, inhibitors targeting the 'B' site are less potent on non-1 HCV genotype NS5B (for review, see De Francesco and Migliaccio (2005)). On the contrary, our hits are smaller than those previously described as 'B' site inhibitors and show a different binding mode. They might exhibit a larger antiviral spectrum through NS5B inhibition on non-1 genotypes naturally resistant to other NNIs targeting the 'B' site.

The docking algorithms have proposed several models for each inhibitor. The 6-xanthone derivatives, for example, could bind the center or the right side of the 'B' site. In order to discriminate between these models several new amino acid mutations were proposed at the central position of the 'B' site, on the basis of a detailed analysis of the docking poses. All the residues that interact with the 6-xanthone compounds are very well conserved in the different genotypes (http://euhcvdb.ibcp.fr/euHCVdb/). We show in this paper that a single mutation of residues lying in the 'B' site deeply affect the expression and/or the activity of recombinant proteins. Interestingly, the R422 residue has been recently shown to be crucial for the replication of subgenomic replicon (Dazert et al., 2009), its mutation leading to an important loss of viral fitness. Structural analysis showed that R422 engaged hydrogen bonds with Y477, and is in a close proximity of W428. These results associated with our failure to express R422A and W508D mutant polymerases, suggest an essential role for this site in both activity and folding of the enzyme. Moreover, results obtained with the Y477F mutant clearly define the 'B' site as a regulator of the transition from the initiation to the elongation phases, involving unknown structural/conformational changes. Our results are in line with those of Biswal et al. (2005, 2006) which showed that upon binding of inhibitors to the 'B' site, movement of helix T could account for the inhibition, and those by Howe et al. (2006) which showed that 'B' site inhibitors impaired the switch to elongation allowing only the synthesis of 5-mer products. It is also worth noting that two studies reporting screening either by fragment based crystallographic (Antonysamy et al., 2008) or by virtual docking (Corbeil et al., 2008) proposed inhibitors centered in the 'B' site and involving interaction with the Tyrosine 477 residue. The substitution of the Tyrosine by a Phenylalanine removes a single hydroxyl group not only involved in hydrogen bonds with Proline 417 and Arginine

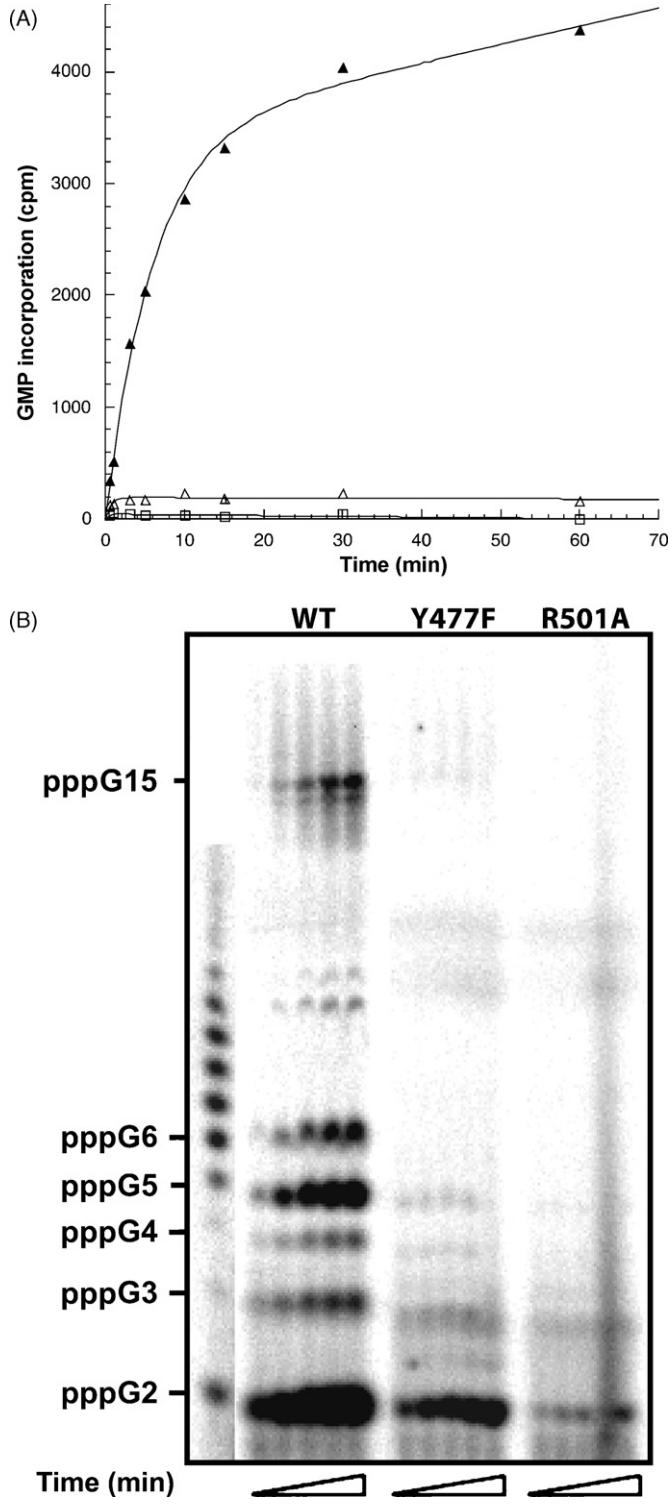


**Fig. 7.** Activities of the WT, Y477F and R501A NS5B on homopolymeric poly(C) or oligo(C) RNA templates. (A) Time course of incorporation of [$^3$H]GTP into poly(C) RNA template by WT (▲) or Y477F (△), and R501A (□) NS5B. RNA synthesis is represented as GMP incorporation into insoluble product (cpm) as a function of time. (B) Kinetic of RNA synthesis using an oligoC RNA template and α-$^{32}$[P]-GTP. Samples were quenched at various times (30 s, 1 min, 5 min, 15 min, 30 min) and RNA products synthesized by WT, Y477F or R501A NS5B were resolved on 14% polyacrylamide/7 M urea gel. RNA markers synthesized using T7 RNA polymerase are indicated on the left.

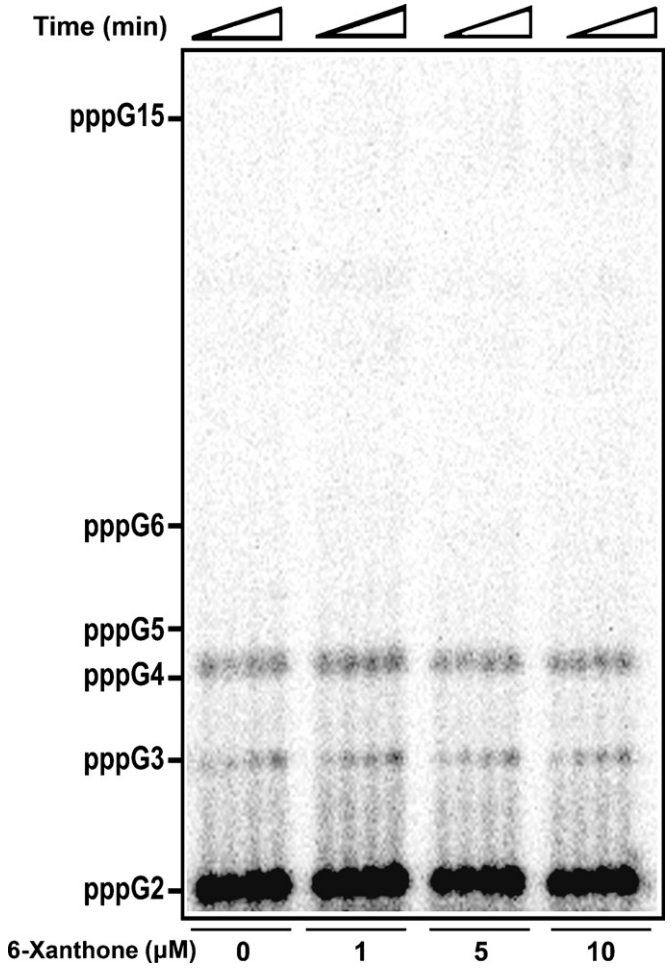


**Fig. 8.** 6-Xanthone does not inhibit Y477F NS5B-mediated dinucleotide synthesis. Time course of GMP incorporation into RNA using an oligo(C) RNA template. Reactions were performed as described in Section 2 using α-$^{32}$P-GTP (1 μCi), Y477F NS5B (1 μM) and 6-xanthone compound **11** (0, 1, 5, or 10 μM). Reaction time course was followed from 1 min to 15 min. RNA products were resolved on 14% acrylamide denaturing gel electrophoresis. Positions of the RNA markers synthesized using T7 RNA polymerase are indicated on the left.

422 (Fig. 9), but also involved (in our model), in the binding of 6-xanthone compounds (Fig. 4B). Because RNA synthesis initiation is barely affected by the Y477F mutation (Table 2), the hydroxyl of Tyrosine 477 has to be engaged into new hydrogen bonds required for the conformational switch to the elongation mode. In light of our results, we propose that the loss of this hydroxyl group by the substitution to a Phenylalanine compromises these new interactions and lock the enzyme into the initiation conformation. Because 6-xanthone compounds could be engaged in a similar interaction with Y477, we infer that they could promote a similar locked conformation accounting for the inhibitory effects of the compounds targeting this site (See Fig. 9 for a more global representation of the environment of the Tyrosine 477). However, 6-xanthone compounds are also able to inhibit the initiation step of RNA synthesis, which is less affected by the Y477F mutation. Inhibition of conformational changes may be one side of the action of 6-xanthone compounds. Direct effect on enzyme activity during initiation may also be required to fully inhibit the polymerase activity. The mechanism of this direct effect on initiation has not yet been identified. Interestingly, all the residues involved in 6-xanthone binding are conserved in all genotypes analyzed so far (Fig. 9). Because their mutation leads to unfolded or barely active proteins *in vitro* and loss of viral fitness in the replicon system (Dazert et al., 2009), we

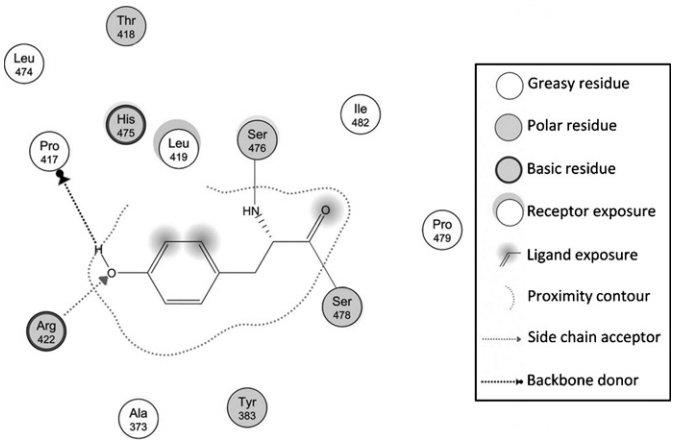


**Fig. 9.** Tyrosine 477 atomic interactions diagram in the protein structure. The Tyrosine 477 hydroxyl is involved in several hydrogen bonds with Arginine 422 and Proline 417. By mutating this Tyrosine to a Phenylalanine, the hydrogen bond network located in the central pocket of the 'B' site is destabilized leading to an inhibition of the enzyme elongation activity. This diagram was generated using the 'ligand interaction' function of the MOE software (Chemcomp company) (Clark and Labute, 2007).

can reasonably propose that the appearance of mutation of such residues upon 6-xanthone treatment might well be reduced and clearly be unfavorable to viral growth. Structural characterization of our model could strengthen our *in silico* predictions and validate the binding mode of this xanthone derivative.

Finally, our results point to a conserved residue in the 'B' site as essential to a conformational change required to engage into processive RNA synthesis. Compounds targeting this central residue might help both the understanding of the role of this essential site and develop new classes of highly potent antiviral compounds.

## Acknowledgments

We would like to thank Laurent Jacquotot and Philippe Vaglio from the Modul-Bio™ start up (www.modul-bio.com) held in Marseille for providing the LIMS used to manage the plates of the chemical library. We thank the "Association pour la Recherche sur le Cancer" (ARC) for financial support to CB and funding allowing the purchase of the automated screening platform; the "Region Provence-Alpes-Côte d'Azur"; the "Université de la Méditerranée" and the "Institut de Chimie des substances Naturelles" (CNRS, Gif-sur-Yvette, France) for financial support. We thank the "GDS Chimiothèque Nationale" for its support in the library setup; Vivalis for initial work on the *in vitro* screening (FCE-Vivalis); and the financial support "Mole ANTI-HEPC: Atlantic Biotherapies No. 2006/83". We also would like to thank James Kwarteng-Amaning for critical reading of the manuscript.

## Appendix A. Supplementary data

Supplementary data associated with this article can be found, in the online version, at doi:10.1016/j.antiviral.2009.06.009.

## References

Antonysamy, S.S., Aubol, B., Blaney, J., Browner, M.F., Giannetti, A.M., Harris, S.F., Hébert, N., Hendle, J., Hopkins, S., Jefferson, E., Kissinger, C., Leveque, V., Marciano, D., McGee, E., Nájera, I., Nolan, B., Tomimoto, M., Torres, E., Wright, T., 2008. Fragment-based discovery of hepatitis C virus NS5b RNA polymerase inhibitors. Bioorg. Med. Chem. Lett. 18, 2990–2995.

Beaulieu, P.L., 2007. Non-nucleoside inhibitors of the HCV NS5B polymerase: progress in the discovery and development of novel agents for the treatment of HCV infections. Curr. Opin. Investig. Drugs 8, 614–634.

Betzi, S., Suhre, K., Chétrit, B., Guerlesquin, F., Morelli, X., 2006. GFscore: a general nonlinear consensus scoring function for high-throughput docking. J. Chem. Inf. Model. 46, 1704–1712.

Biswal, B.K., Cherney, M.M., Wang, M., Chan, L., Yannopoulos, C.G., Bilimoria, D., Nicolas, O., Bedard, J., James, M.N., 2005. Crystal structures of the RNA-dependent RNA polymerase genotype 2a of hepatitis C virus reveal two conformations and suggest mechanisms of inhibition by non-nucleoside inhibitors. J. Biol. Chem. 280, 18202–18210.

Biswal, B.K., Wang, M., Cherney, M.M., Chan, L., Yannopoulos, C.G., Bilimoria, D., Bedard, J., James, M.N., 2006. Non-nucleoside inhibitors binding to hepatitis C virus NS5B polymerase reveal a novel mechanism of inhibition. J. Mol. Biol. 361, 33–45.

Bougie, I., Charpentier, S., Bisaillon, M., 2003. Characterization of the metal ion binding properties of the hepatitis C virus RNA polymerase. J. Biol. Chem. 278, 3868–3875.

Bressanelli, S., Tomei, L., Rey, F.A., De Francesco, R., 2002. Structural analysis of the hepatitis C virus RNA polymerase in complex with ribonucleotides. J. Virol. 76, 3482–3492.

Butcher, S.J., Grimes, J.M., Makeyev, E.V., Bamford, D.H., Stuart, D.I., 2001. A mechanism for initiating RNA-dependent RNA polymerisation. Nature 410, 235–240.

Clark, A.M., Labute, P., 2007. 2D depiction of protein–ligand complexes. J. Chem. Inf. Model. 47, 1933–1944.

Clark, R.D., Strizhev, A., Leonard, J.M., Blake, J.F., Matthew, J.B., 2002. Consensus scoring for ligand/protein interactions. J. Mol. Graph. Model. 20, 281–295.

Corbeil, C.R., Englebienne, P., Yannopoulos, C.G., Chan, L., Das, S.K., Bilimoria, D., L'Heureux, L., Moitessier, N., 2008. Docking ligands into flexible and solvated macromolecules. 2. Development and application of fitted 1.5 to the virtual screening of potential HCV polymerase inhibitors. J. Chem. Inf. Model. 48, 902–909.

Dazert, E., Neumann-Haefelin, C., Bressanelli, S., Fitzmaurice, K., Kort, J., Timm, J., McKiernan, S., Kelleher, D., Gruener, N., Tavis, J.E., Rosen, H.R., Shaw, J., Bowness, P., Blum, H.E., Klenerman, P., Bartenschlager, R., Thimme, R., 2009. Loss of viral fitness and cross-recognition by CD8+ T cells limit HCV escape from a protective HLA-B27-restricted human immune response. J. Clin. Invest. 119, 376–386.

De Francesco, R., Carfi, A., 2007. Advances in the development of new therapeutic agents targeting the NS3-4A serine protease or the NS5B RNA-dependent RNA polymerase of the hepatitis C virus. Adv. Drug Deliv. Rev. 59, 1242–1262.

De Francesco, R., Migliaccio, G., 2005. Challenges and successes in developing new therapies for hepatitis C. Nature 436, 953–960.

Di Marco, S., Volpari, C., Tomei, L., Altamura, S., Harper, S., Narjes, F., Koch, U., Rowley, M., De Francesco, R., Migliaccio, G., Carfi, A., 2005. Interdomain communication in hepatitis C virus polymerase abolished by small molecule inhibitors bound to a novel allosteric site. J. Biol. Chem. 280, 29765–29770.

Dutartre, H., Boretto, J., Guillemot, J.C., Canard, B., 2005. A relaxed discrimination of 2′-O-methyl-GTP relative to GTP between de novo and elongative RNA synthesis by the hepatitis C RNA-dependent RNA polymerase NS5B. J. Biol. Chem. 280, 6359–6368.

Dutartre, H., Bussetta, C., Boretto, J., Canard, B., 2006. General catalytic deficiency of hepatitis C virus RNA polymerase with an S282T mutation and mutually exclusive resistance towards 2′-modified nucleotide analogues. Antimicrob. Agents Chemother. 50, 4161–4169.

Howe, A.Y., Cheng, H., Thompson, I., Chunduru, S.K., Herrmann, S., O'Connell, J., Agarwal, A., Chopra, R., Del Vecchio, A.M., 2006. Molecular mechanism of a thumb domain hepatitis C virus nonnucleoside RNA-dependent RNA polymerase inhibitor. Antimicrob. Agents Chemother. 50, 4103–4113.

Ikegashira, K., Oka, T., Hirashima, S., Noji, S., Yamanaka, H., Hara, Y., Adachi, T., Tsuruha, J., Doi, S., Hase, Y., Noguchi, T., Ando, I., Ogura, N., Ikeda, S., Hashimoto, H., 2006. Discovery of conformationally constrained tetracyclic compounds as potent hepatitis C virus NS5B RNA polymerase inhibitors. J. Med. Chem. 49, 6950–6953.

Koch, U., Attenni, B., Malancona, S., Colarusso, S., Conte, I., Di Filippo, M., Harper, S., Pacini, B., Giomini, C., Thomas, S., Incitti, I., Tomei, L., De Francesco, R., Altamura, S., Matassa, V.G., Narjes, F., 2006. 2-(2-Thienyl)-5,6-dihydroxy-4-carboxypyrimidines as inhibitors of the hepatitis C virus NS5B polymerase: discovery, SAR, modeling, and mutagenesis. J. Med. Chem. 49, 1693–1705.

Kramer, B., Rarey, M., Lengauer, T., 1999. Evaluation of the FLEXX incremental construction algorithm for protein–ligand docking. Proteins 37, 228–241.

Lee, G., Piper, D.E., Wang, Z., Anzola, J., Powers, J., Walker, N., Li, Y., 2006. Novel inhibitors of hepatitis C virus RNA-dependent RNA polymerases. J. Mol. Biol. 357, 1051–1057.

Love, R.A., Parge, H.E., Yu, X., Hickey, M.J., Diehl, W., Gao, J., Wriggers, H., Ekker, A., Wang, L., Thomson, J.A., Dragovich, P.S., Fuhrman, S.A., 2003. Crystallographic identification of a noncompetitive inhibitor binding site on the hepatitis C virus NS5B RNA polymerase enzyme. J. Virol. 77, 7575–7581.

Ludmerer, S.W., Graham, D.J., Boots, E., Murray, E.M., Simcoe, A., Markel, E.J., Grobler, J.A., Flores, O.A., Olsen, D.B., Hazuda, D.J., LaFemina, R.L., 2005. Replication fitness and NS5B drug sensitivity of diverse hepatitis C virus isolates characterized by using a transient replication assay. Antimicrob. Agents Chemother. 49, 2059–2069.

Luo, G., Hamatake, R.K., Mathis, D.M., Racela, J., Rigat, K.L., Lemm, J., Colonno, R.J., 2000. De novo initiation of RNA synthesis by the RNA-dependent RNA polymerase (NS5B) of hepatitis C virus. J. Virol. 74, 851–863.

Ma, H., Leveque, V., De Witte, A., Li, W., Hendricks, T., Clausen, S.M., Cammack, N., Klumpp, K., 2005. Inhibition of native hepatitis C virus replicase by nucleotide and non-nucleoside inhibitors. Virology 332, 8–15.

Morris, G.M., Goodsell, D.S., Huey, R., Olson, A.J., 1996. Distributed automated docking of flexible ligands to proteins: parallel applications of AutoDock 2.4. J. Comput. Aided Mol. Des. 10, 293–304.

Ng, K.K., Arnold, J.J., Cameron, C.E., 2008. Structure–function relationships among RNA-dependent RNA polymerases. Curr. Top. Microbiol. Immunol. 320, 137–156.

Nicolas, O., Boivin, I., St-Denis, C., Bedard, J., 2008. Genotypic analysis of HCV NS5B variants selected from patients treated with VCH-759, and viral load declines. In: 43rd Annual Meeting of the European Association for the Study of the Liver, Milan, Italy.

Pauwels, F., Mostmans, W., Quirynen, L.M., van der Helm, L., Boutton, C.W., Rueff, A.S., Cleiren, E., Raboisson, P., Surleraux, D., Nyanguile, O., Simmen, K.A., 2007. Binding-site identification and genotypic profiling of hepatitis C virus polymerase inhibitors. J. Virol. 81, 6909–6919.

Pfefferkorn, J.A., Greene, M.L., Nugent, R.A., Gross, R.J., Mitchell, M.A., Finzel, B.C., Harris, M.S., Wells, P.A., Shelly, J.A., Anstadt, R.A., Kilkuskie, R.E., Kopta, L.A., Schwende, F.J., 2005. Inhibitors of HCV NS5B polymerase. Part 1: evaluation of the southern region of (2Z)-2-(benzoylamino)-3-(5-phenyl-2-furyl)acrylic acid. Bioorg. Med. Chem. Lett. 15, 2481–2486.

Powers, J.P., Piper, D.E., Li, Y., Mayorga, V., Anzola, J., Chen, J.M., Jaen, J.C., Lee, G., Liu, J., Peterson, M.G., Tonn, G.R., Ye, Q., Walker, N.P., Wang, Z., 2006. SAR and mode of action of novel non-nucleoside inhibitors of hepatitis C NS5b RNA polymerase. J. Med. Chem. 49, 1034–1046.

Rarey, M., Kramer, B., Lengauer, T., 1999. The particle concept: placing discrete water molecules during protein–ligand docking predictions. Proteins 34, 17–28.

Rarey, M., Kramer, B., Lengauer, T., Klebe, G., 1996. A fast flexible docking method using an incremental construction algorithm. J. Mol. Biol. 261, 470–489.

Somsouk, M., Lauer, G.M., Casson, D., Terella, A., Day, C.L., Walker, B.D., Chung, R.T., 2003. Spontaneous resolution of chronic hepatitis C virus disease after withdrawal of immunosuppression. Gastroenterology 124, 1946–1949.

Tomei, L., Altamura, S., Bartholomew, L., Biroccio, A., Ceccacci, A., Pacini, L., Narjes, F., Gennari, N., Bisbocci, M., Incitti, I., Orsatti, L., Harper, S., Stansfield, I., Rowley, M., De Francesco, R., Migliaccio, G., 2003. Mechanism of action and antiviral activity of benzimidazole-based allosteric inhibitors of the hepatitis C virus RNA-dependent RNA polymerase. J. Virol. 77, 13225–13231.

Tomei, L., Altamura, S., Bartholomew, L., Bisbocci, M., Bailey, C., Bosserman, M., Cellucci, A., Forte, E., Incitti, I., Orsatti, L., Koch, U., De Francesco, R., Olsen, D.B., Carroll, S.S., Migliaccio, G., 2004. Characterization of the inhibition of hepatitis C virus RNA replication by nonnucleosides. J. Virol. 78, 938–946.